Incomplete fusion in the $^{19}F+^{93}Nb$ reaction

B. S. Tomar, A. Goswami, G. K. Gubbi, A. V. R. Reddy, and S. B. Manohar
Radiochemistry Division, Bhabha Atomic Research Centre, Mumbai 400 085, India

Bency John and S. K. Kataria
Nuclear Physics Division, Bhabha Atomic Research Centre, Mumbai 400 085, India

(Received 3 March 1998)

The kinetic energy spectra and angular distributions of projectilelike fragments were measured by silicon based ΔE-E telescopes in 95 MeV $^{19}F+^{93}Nb$. The spectra of oxygen and nitrogen fragments show the existence of two reaction mechanisms, namely, quasielastic transfer and incomplete fusion reactions. On the other hand, the carbon and other lower Z fragments show broad Gaussian spectra indicative of incomplete fusion reactions only. The quasielastic transfer is explained in terms of the direct surface transfer model. The cross sections of complete and incomplete fusion channels agree with the calculations based on the sum-rule model. Recoil range distributions of evaporation residues formed in the 95 MeV $^{19}F+^{93}Nb$ reaction were measured using recoil catcher and off-line gamma-ray spectrometry. The results corroborate the binary nature of the incomplete fusion reactions. [S0556-2813(98)06212-8]

PACS number(s): 25.70.Jj, 25.70.Mn

I. INTRODUCTION

The main attraction to study heavy ion reactions is to unfold the multiplicity of processes involved and their evolution with variation in the entrance channel parameters, namely, beam energy, angular momentum, and entrance channel mass asymmetry. With low Z heavy ions as projectile, compound nucleus formation is accepted as the major reaction mechanism, at least for beam energies up to 10 MeV/nucleon. Since the early sixties, when Kaufmann *et al.* [1] observed reactions involving transfer of a large number of nucleons from projectile to target, researchers [2–6] have focused their attention on the formation of projectile like fragments (PLF's) in the low Z heavy ion induced reactions at beam energies below 10 MeV/nucleon. Kaufmann's work is now explained in terms of the deep inelastic collisions (DIC), which are binary reactions with considerable amount of energy damping [7]. Later studies on DIC were carried out with heavier projectiles and targets where the cross sections for such processes are much higher. Light heavy ion induced reactions, on the other hand, were explored to obtain the information about the formation of PLF's particularly in the energy domain of 10–30 MeV/nucleon. General conclusions from such studies are that the PLF's are formed with approximately beam velocity at forward angles, and their angular distribution peaking at grazing angle [8,9]. Terms like incomplete fusion (ICF), massive transfer reactions, quasielastic transfer (QET) reactions, etc. have been used to describe these processes. The sum rule model of Wilczynski [5] explains ICF in terms of reactions with angular momenta above the critical angular momentum (l_{CR}) for complete fusion of projectile and target. Udagawa and Tamura [10] explained the shapes of particle spectra and the angular distributions of fast alpha particles in terms of break up fusion model based on DWBA. Experimental studies on ICF have shown that ICF probability depends on the entrance channel mass asymmetry [11,12] and it is associated with peripheral collisions [13,14]. However, the basic question remains whether separate mechanism operates for these type of reactions or they are same as DIC. Mermaz *et al.* [15], Gelbke *et al.* [6], and Balster *et al.* [16] carried out extensive work on the formation of PLF's in low Z heavy ion induced reactions in the beam energy range of 10 MeV/nucleon . It was concluded from these studies that basically three reaction mechanisms operate in the formation of PLF, namely, quasielastic transfer reactions, deep inelastic collisions and compound nucleus like mechanism. Recently Zagrabaev [17] tried to explain these reactions in terms of direct multistep processes that include QET as well as the reactions with large transfer of mass, energy and angular momentum. However, a clear understanding about the mechanism of the formation of these PLF's is yet to emerge. In the present work we report our results on inclusive measurements of energy spectra and angular distribution of PLF's by silicon based telescopes in 95 MeV $^{19}F+^{93}Nb$. The recoil range distributions (RRD) of evaporation residues were measured by off-line gamma-ray spectrometry to ascertain the binary nature of the reactions leading to PLF's. The results are discussed in the light of the existence of different reaction mechanisms leading to the formation of PLF's. In Sec. II the details of the experiments on measurements of the energy spectra and the angular distributions of PLF's as well as the recoil range distribution of evaporation residues (ER's) are described. The results of the present work are presented and discussed in Sec. III. The conclusions drawn from the present study are listed in Sec. IV.

II. EXPERIMENTAL DETAILS

The experiments were carried out using the BARC-TIFR pelletron facility at Mumbai. The measurements of PLF's were carried out using the one meter diameter scattering chamber of the pelletron facility using ΔE-E telescopes based on surface barrier silicon detectors. The experiments on RRD were carried out by recoil catcher technique followed by direct gamma-ray spectrometry.

A. Projectilelike fragments

A self-supporting rolled niobium foil of 450 $\mu g/cm^2$ thickness was used as target. The measurements were carried out with a ^{19}F beam with an energy of 95 MeV. The detection system consisted of two well collimated silicon based ΔE-E telescopes mounted in the reaction plane. The PLF's with Z in the range $2 \leqslant Z \leqslant 8$ were detected using two ΔE-E telescopes ($T1$ and $T2$). The telescope $T1$ comprised of a 22.8 μm ΔE detector and a 1 mm E detector. The telescope $T2$ comprised of a 17 μm ΔE detector and a 1 mm E detector. The solid angle subtended by $T1$ and $T2$ telescopes was 1.62 msr. The absolute cross sections were determined by normalization to Rutherford scattering using a monitor counter at θ_{lab} of 20°. The measurements were carried out in the angular range between 20° and 160°. The energy calibration of the telescopes was carried out using a ^{239}Pu-^{241}Am composite alpha source as well as the elastically scattered ^{19}F ions detected at forward angles. The purity of the niobium target was ascertained by absence of elastic recoil peaks corresponding to impurity elements in the spectra. The data on alpha particles and protons have been reported in a separate paper [18] and hence are not discussed here.

B. Recoil range distributions

For the measurement of recoil range distribution (RRD) of evaporation residues, niobium targets of thickness around 100 $\mu g/cm^2$, vacuum evaporated onto 100 $\mu g/cm^2$ thick aluminium foils were used. Duration of irradiation was 16 h. The recoiling ER's were stopped in a stream of 15 aluminium foils of thickness around 100 $\mu g/cm^2$. The thickness of the catcher foils were measured by the energy loss method using a ^{241}Am alpha source and the range energy table of Northcliffe and Schilling [19]. The typical error on the thickness is around 5%. After the irradiation each aluminium foil was counted for the gamma activity of the ER's for two weeks using an efficiency calibrated HPGe detector coupled to a PC based 4 K MCA. The resolution of the detector was 2.0 keV at 1408 keV gamma energy of ^{152}Eu. The analysis of the gamma ray spectra was carried out using the PC version of the peak fitting program SAMPO. The details of the calculation of RRD from the measured count rates are given in [12].

III. RESULTS AND DISCUSSION

A. Kinetic energy spectra

The measured energy spectra of PLF's were transformed into the center of mass (c.m.) coordinate system using the standard kinematic relationships. The c.m. energy spectra of oxygen and nitrogen isotopes are shown in Figs. 1 and 2, respectively. The maxima in the spectra for a given isotope occur at the same energy for all angles and are close to the Q_{opt} for binary l-matched reactions, calculated using the formula used by Wilczynski *et al.* [5]. The kinetic energies corresponding to Q_{opt} are shown by an arrow. The kinetic energy corresponding to the exit channel Coulomb energy (V_c) is also shown by an arrow. Such two component spectra have been obtained by other groups [15,21,22]. However, various groups interpreted their results in different ways. Mermaz *et al.* [15] explained the low energy component in terms of

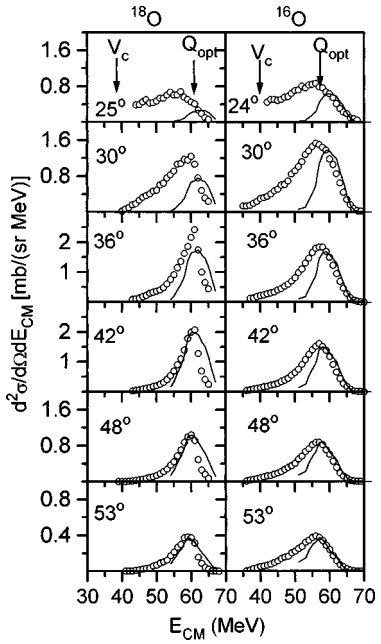

FIG. 1. Center of mass energy spectra of oxygen isotopes in 95 MeV $^{19}F+^{93}Nb$. The angles indicated are CM angles. The solid lines represent the energy spectra calculated using the FAST code for QET. The kinetic energies corresponding to Q_{opt} and V_c for the exit channel are shown by arrows.

DIC with the yields of PLF's following Volkov's Q_{gg} systematics [20]. Parker *et al.* [21] attributed the low energy tails in the energy spectra to the incomplete fusion reactions. Brondi *et al.* [22], on the other hand, identified the QET component as ICF and the low energy tail due to DIC. The existence of narrow high energy component and broad low energy component in the PLF spectra are reminiscent of the Wilczynski diagram in which the kinetic energy spectrum of PLF's at an angle arises from near site as well as far site

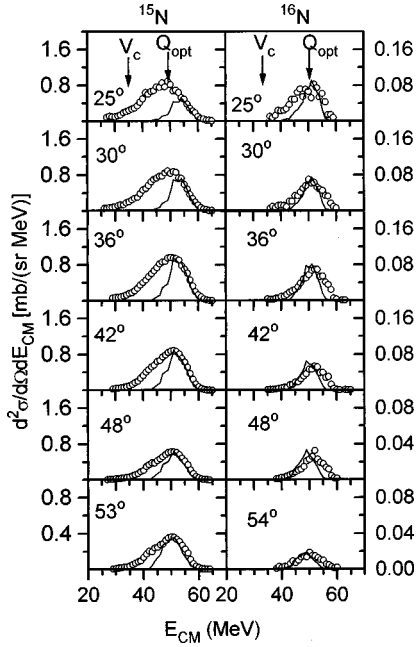

FIG. 2. Center of mass energy spectra of nitrogen isotopes in 95 MeV $^{19}F+^{93}Nb$. The explanations are the same as in Fig. 1.

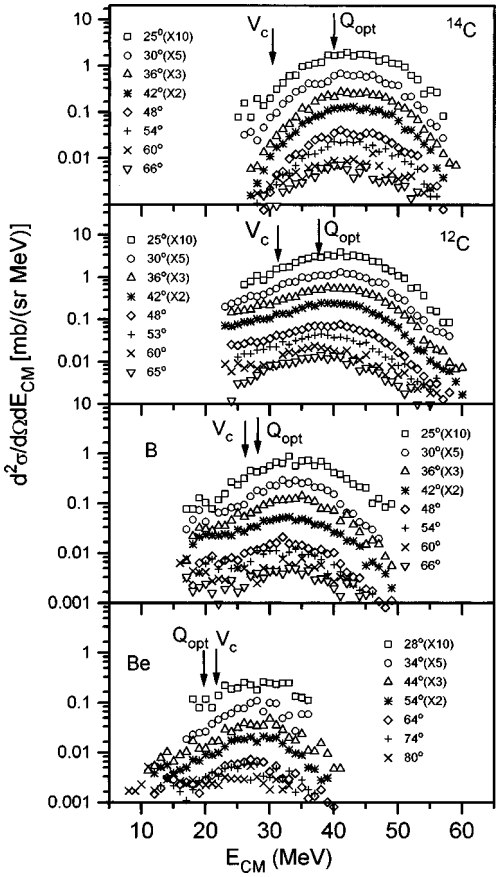

FIG. 3. Center of mass energy spectra of carbon and other lower Z fragments in 95 MeV $^{19}F+^{93}Nb$. The kinetic energies corresponding to Q_{opt} and V_c for the exit channel are shown as arrows.

scattering [7]. The near site scattering results from quasielastic transfer reactions involving very little transfer of energy from the entrance channel into that of the products. The resultant kinetic energy spectra are rather narrow with peak energies close to Q_{opt}. The far site scattering, on the other hand, results from deep inelastic collisions involving considerable amount of damping of initial kinetic energy and angular momentum. The resultant kinetic energy spectra are therefore broad and extend down to Coulomb barrier of the exit channel (V_c) and have forward peaked angular distributions. In this paper we follow the convention of Galin *et al.* [3] and call the dissipative component in the energy spectra of PLF's as arising from ICF reactions, to distinguish them from QET reactions.

The c.m. energy spectra of carbon, boron and beryllium isotopes are shown in Fig. 3. There is a qualitative change in the spectral pattern of these PLF's as compared to those of oxygen and nitrogen isotopes. Unlike spectra of oxygen and nitrogen isotopes, the energy spectra of these isotopes are broad Gaussians in nature. The existence of two reaction mechanisms cannot be concluded from the spectra due to closeness of the energy corresponding to Q_{opt} for QET and the exit channel V_c.

Direct surface transfer reaction model calculations for QET products

The $d^2\sigma/dEd\Omega$ of PLF's were calculated theoretically in the framework of the diffractional model for surface transfer reactions based on the DWBA formalism of Mermaz *et al.* [15] using the code FAST. The input parameters in the calculations are the elastic scattering radius (r_0), the corresponding diffusivity (d) and the amplitude of the nuclear phase in the nuclear elastic scattering phase shift. However, instead of the nuclear phase amplitude the difference between nuclear and Coulomb rainbow angles ($\Delta\theta$) is used in the calculation. These parameters were fixed by fitting the experimental elastic scattering data on $^{19}F+^{93}Nb$ measured in a separate experiment [18]. The values obtained were 1.525 fm, 0.35 fm, and -0.165 radians. In view of the strong attenuation of the nuclear rainbow in the deflection function [15], the calculations were carried out for higher value of $\Delta\theta$. The agreement between the experimental and calculated data was obtained for $\Delta\theta=-0.3$ radians. Similar observations were made by Pagano *et al.* [23] in $^{16}O+^{238}U$ system. As the spectroscopic form factors of the continuum states could not be supplied in the code, the calculations donot give the absolute cross sections of PLF's. The peak energy in the calculated energy spectra were therefore normalized with the corresponding energy in the experimental spectra. The calculated kinetic energy spectra of oxygen and nitrogen isotopes are shown in Figs. 1 and 2 as solid curves. The calculated energy spectra reproduce the high energy part of the experimental energy spectra. In the case of ^{16}N the calculated spectra nearly reproduce the experimental spectra indicating that this isotope is predominantly formed in QET reaction. Similar calculations failed to give any appreciable cross sections for carbon and other lower Z isotopes. This shows that these isotopes are formed only in incomplete fusion reactions. Comparison of calculated spectra with the experimental spectra thus indicates the existence of two components in the energy spectra of oxygen and nitrogen isotopes. The ICF component was extracted by subtracting the normalized QET component from the experimental spectra.

B. Angular distributions

The angular distributions of the QET component in oxygen and nitrogen isotopes and ICF component in all the PLF's are plotted in Fig. 4. The angular distribution of QET component is peaked at grazing angle, while that of the ICF component is forward peaked. The falling $d\sigma/d\Omega$ of ^{18}O and ^{16}O at the most forward angle in the case of ICF component is due to the low energy cut off in the two dimensional ΔE-E spectra. The gradual change of angular distribution as a function of Z indicates a continuous evolution of the reaction mechanism from QET to more dissipative reactions. At present there is no model which can quantitatively explain the energy spectra and angular distributions of the PLF's formed in ICF reactions.

Figure 5 shows the plot of the mean and the width of the c.m. energy spectra of QET and ICF components of the PLF's as a function of their c.m. angle of emission. The mean kinetic energies of both the components remains constant as a function of c.m. angle indicating the binary nature of the collisions leading to the formation of these PLF's. The mean kinetic energy of the QET component is higher than that of the ICF component. The width of the QET component is much smaller than that of the ICF component. Lower mean kinetic energy and higher width of the ICF component

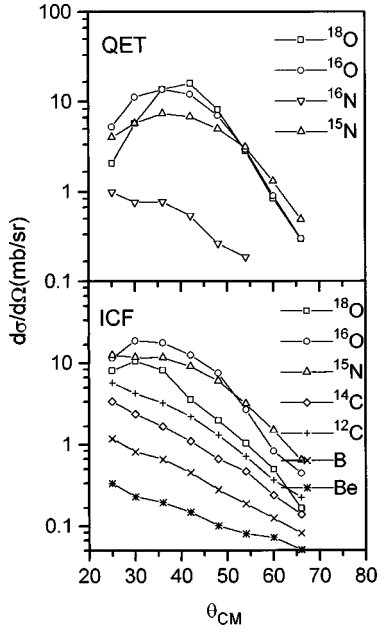

FIG. 4. Angular distribution of PLF's formed in QET (top) and ICF (bottom) reactions.

compared to the QET component indicates dissipation of initial kinetic energy into excitation energy of the products. However this excitation energy will be shared predominantly by the heavier reaction products considering that the excitation energy is shared in the ratio of their masses.

C. PLF yields

Table I gives the yields of the ejectiles obtained by integrating the angular distribution over the angular range of 5–65°. Also shown is the CF cross section obtained from the evaporation residues data [18]. The data below 20° was obtained by extrapolating the experimental angular distribution to 5°. There is a gradual decrease in cross section as we move away from the projectile atomic number. It is interesting to note that the cross section for ^{16}O is much higher than ^{18}O which reflects the effect of Q_{gg} as seen from Table I. Formation of ^{16}O is also possible in sequential-break up reactions, namely, proton pick up by projectile from target to produce ^{20}Ne followed by break up of the latter into ^{16}O and an alpha particle. Sequential breakup yields increase with increasing beam energy. However at the beam energies of the present work the cross section for such events is expected to be small [16]. Figure 6 shows a plot of the ratio of experimental cross section to that calculated using the Mermaz model against the number of nucleons transferred from projectile to target at 35° laboratory angle which is the grazing angle. The straight line shows linear fit to the data on ^{18}O, ^{16}O, and ^{16}N. This ratio is directly proportional to the mean product of the entrance and exit channel spectroscopic form factors. For sequential nucleon transfer reaction mechanism this ratio should fall by one order of magnitude for every nucleon transferred. The ratio for ^{15}N lies much above the linear fit indicating the role of cluster transfer in the formation of this isotope.

TABLE I. Integrated cross sections for PLF's formed in 95 MeV $^{19}F+^{93}Nb$.

Fragment	Q_{gg}	σ(mb) (expt.)	σ(mb) (sum rule)
^{18}O	0.498	20.6±0.4	1.7
^{17}O	−0.179	14.1±0.3	1.4
^{16}O	4.832	35.3±0.7	5.8
^{16}N	−8.56	1.92±0.2	0.5
^{15}N	−1.576	27.1±1.3	3.5
^{14}N	−5.131	3.53±0.18	1.3
^{14}C	−3.492	4.28±0.21	8.3
^{13}C	−4.205	6.03±0.31	6.8
^{12}C	0.522	10.61±0.51	26.2
^{11}B	−9.955	1.37±0.07	5.6
^{10}B	−13.926	0.25±0.03	1.8
^{10}Be	−13.386	0.16±0.02	5.3
^{9}Be	−12.573	0.43±0.04	6.9
^{7}Be	−16.049	0.08±0.01	2.3
Complete fusion		1220±93	1181

Sum-rule model calculations

Since the fast code does not calculate the absolute cross sections of PLF's, we compared the experimental cross sections with those calculated using the sum rule model which

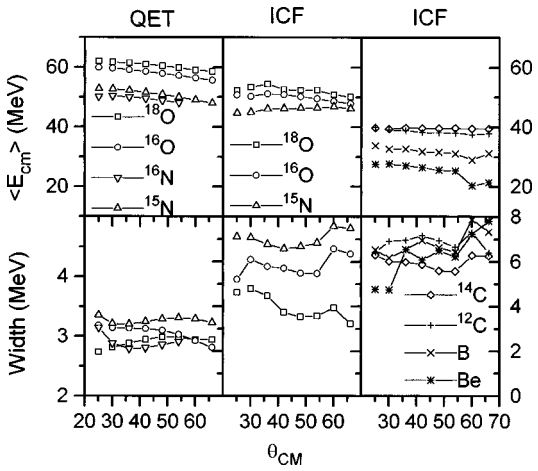

FIG. 5. Plot of mean and width of the CM kinetic energy spectra of QET and ICF products.

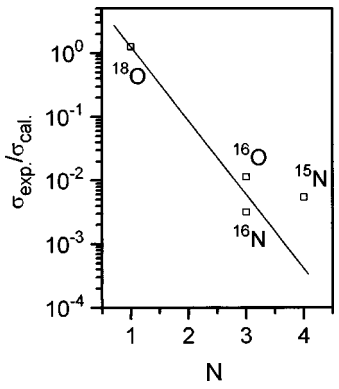

FIG. 6. Plot of the ratio of experimental cross section to that calculated using FAST code at $\theta_{lab.}=35°$. The solid line is the linear fit to the data of ^{18}O, ^{16}O, and ^{16}N.

combines the partial statistical equilibrium model of Bondorf *et al.* [24] with the concept of localization of various ICF channels in angular momentum space above the critical angular momentum for complete fusion. The cross section for a reaction channel is given by [5]

$$\sigma(i)=\pi\lambda^2\sum_{l=0}^{l_{\max}}(2l+1)\,\frac{T_l(i)p(i)}{\Sigma_j T_l(j)p(j)}, \tag{1}$$

where $p(i)$ is the reaction probability for a given channel and is given by

$$p(i)\propto e^{[Q_{gg}(i)-Q_c(i)]/T}. \tag{2}$$

$Q_{gg}(i)$ is the ground state Q value. $Q_c(i)$ is the change in the Coulomb interaction energy due to transfer of charge, which is calculated using the expression,

$$Q_c(i)=(Z_3Z_4-Z_1Z_2)/R_c, \tag{3}$$

where R_c represents an effective relative distance where the transfer of charge takes place. The subscripts 1,2 and 3,4 refer to entrance and exit channels, respectively. T is an effective temperature parameter which is a measure of the temperature at the hot contact zone. The transmission coefficient (T_l) are assumed to have a smooth functional form as

$$T_l(i)=\left[1+\exp\left(\frac{l-l_{\lim}(i)}{\Delta}\right)\right]^{-1}. \tag{4}$$

Δ describes the diffuseness of the cutoff in the T_l distribution. The input parameters R_c, Δ and T used in the calculations were 1.5 $(A_1^{1/3}+A_2^{1/3})$, 1.7 $\hbar$ and 3.5 MeV, respectively as used by Wilczynski *et al.* [5]. The limiting angular momentum for a given channel was calculated from the critical angular momentum for fusion of the part of the projectile with the target. The critical angular momentum (l_{CR}) for complete fusion of two nuclei was calculated using the formula given in Ref. [5]. The l_{CR} for the entrance channel was obtained from the experimentally measured CF cross section [18] which was found to be 1220 ± 93 mb. The corresponding l_{CR} is $39\hbar$. The summation of Eq. (1) was carried out up to $l_{\max}$ which was calculated from the reaction cross section (1510 ± 90) obtained from experimental elastic scattering data [18]. The corresponding $l_{\max}$ value is $52\hbar$. The cross sections calculated using the sum-rule model are shown in Table I. Though the calculated values agree with the experimental values in the case of CF, for other PLF's large deviations are observed. However, the trends of the cross sections with the Q_{gg} values can be seen in both experimental as well as calculated values. The largest discrepancy arises in the case of PLF's which are close to the projectile, namely, oxygen and nitrogen isotopes. This is obvious as these PLF's are formed in direct transfer reactions as discussed above.

D. Recoil range distributions

Recoil range distributions provide information about the extent of linear momentum transfer from projectile in the formation of a particular reaction product. The RRD's for several ER's are plotted in Fig. 7 for 95 MeV ^{19}F beam energy. The RRD's for indium isotopes show narrow Gaussian curves with mean range corresponding to full momentum transfer. The RRD's were also calculated for decay of the CN (^{112}Sn) formed in CF using the code PACE2 [25]. The details about the simulation of RRD's using PACE2 code are given in [12]. The input parameters used in PACE2 calculations were the same as used in reproducing the excitation function data in [18]. The calculated values agree with experimental RRD's for indium isotopes. For ^{105}Ag and ^{101}Rh, the experimental RRD shows a low range component. The RRD's of ^{97}Ru and ^{95,96}Tc show ranges much lower than that expected for CF, indicating that they are formed in ICF reactions. The possible ICF reactions that can give rise to these products are

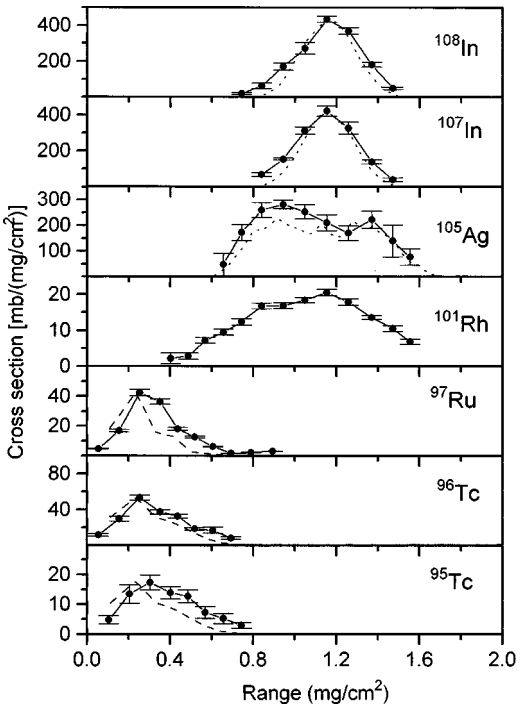

FIG. 7. Recoil range distribution of evaporation residues in 95 MeV ^{19}F+^{93}Nb. The solid lines are eye guides to the experimental data. The dotted lines are the simulated RRD's for CF products. The dashed lines are the RRD's simulated from $d^2\sigma/dEd\Omega$ of complementary fragments.

$$^{93}\mathrm{Nb}(^{19}\mathrm{F},^{13}\mathrm{C})^{99}\mathrm{Ru}^* \text{ and } ^{93}\mathrm{Nb}(^{19}\mathrm{F},^{15}\mathrm{N})^{97}\mathrm{Tc}^*.$$

The excited intermediate nuclei ^{99}Ru and ^{97}Tc may subsequently deexcite by neutron emission to form ^{97}Ru, and ^{95,96}Tc. Observations of PLF's such as ^{13}C, ^{15}N, etc. show the occurrence of such reactions. However, many targetlike residues formed in similar type of ICF reactions could not be measured due to lack of suitable decay schemes, that is, half life and gamma ray intensity. The ranges of technetium products could be reproduced by kinematically transforming the $d^2\sigma/dEd\Omega$ of ^{15}N fragments into that of technetium products. These RRD's are shown as dashed lines in the RRD curves for technetium products. The agreement between the experimental RRD and that simulated from the data of ^{15}N indicates that they are the complementary products of a binary reaction.

IV. CONCLUSION

The present study has shown that, apart from complete fusion of projectile and target nuclei forming a compound nucleus, two other mechanisms occur, namely, (i) quasielastic transfer reactions leading to projectile like fragments with narrow angular distributions peaked sideways and the kinetic energy spectra peaking at Q_{opt} for binary *l*-matched reactions and (ii) a more dissipative incomplete fusion reaction in which a large part of the projectile is transferred to the target nucleus with considerable amount of energy damping and emission of the remaining part of the projectile preferentially at forward angles.

ACKNOWLEDGMENTS

The authors thank D. C. Ephraim for preparation of thin targets and catcher foils. Thanks are also due to the operating personnel of the Pelletron facility for their cooperation during the experiment. We are grateful to Professor M. C. Mermaz for providing us with a copy of the code FAST. It is a pleasure to acknowledge the initial efforts of Aruna Nijasure in this work.

[1] R. Kaufmann and R. Wolfgang, Phys. Rev. **121**, 192 (1961).
[2] H. C. Britt and A. R. Quinton, Phys. Rev. **124**, 8/77 (1961).
[3] J. Galin, B. Gatty, M. Lefort, J. Peter, X. Tarrago, and R. Basile, Nucl. Phys. **A159**, 161 (1970).
[4] T. Inamura, M. Ishihara, T. Fukuda, T. Shimoda, and H. Hiruta, Phys. Lett. **68B**, 51 (1977).
[5] J. Wilczynski, K. Siwek-Wilczynska, J. Van Driel, S. Gonggrijp, D. C. J. M. Hageman, R. V. F. Janssens, J. Lukasiak, R. H. Siemssen, and S. Y. Van der Werf, Nucl. Phys. **A373**, 109 (1982).
[6] C. K. Gelbke, D. K. Scott, M. Bini, D. L. Hendrie, J. L. Laville, J. Mahoney, M. C. Mermaz, and C. Olmer, Phys. Lett. **70B**, 415 (1977).
[7] M. Lefort and Ch. Ngo, Ann. Phys. (N.Y.) **3**, 5 (1978).
[8] R. H. Siemssen, Nucl. Phys. **A400**, 245c (1983).
[9] Ch. Ngo, Prog. Part. Nucl. Phys. **16**, 139 (1985).
[10] T. Udagawa and T. Tamura, Phys. Rev. Lett. **45**, 1311 (1980).
[11] H. Morgenstern, W. Bohne, W. Galster, and K. Grabisch, Phys. Rev. Lett. **52**, 1104 (1984).
[12] B. S. Tomar, A. Goswami, A. V. R. Reddy, S. K. Das, P. P. Burte, S. B. Manohar, and Bency John, Phys. Rev. C **49**, 941 (1994).
[13] W. Traumann, O. Hansen, H. Tricoire, W. Hering, R. Ritzka, and W. Trombik, Phys. Rev. Lett. **53**, 1630 (1984).
[14] B. Bindukumar, S. Mukherjee, S. Chakrabarty, B. S. Tomar, A. Goswami, and S. B. Manohar, Phys. Rev. C **57**, 743 (1998).
[15] M. C. Mermaz, R. Dayras, J. Barrette, B. Berthier, D. M. De Castro Rizzo, O. Cisse, R. Legrain, A. Pagano, E. Pollacco, H. Delgrange, W. Mittig, B. Heusch, G. Langano, and A. Palmeri, Nucl. Phys. **A441**, 129 (1985).
[16] G. J. Balster, H. W. Wilschut, R. H. Siemssen, P. C. N. Crouzen, P. B. Goldhoorn, and Z. Sujkowski, Nucl. Phys. **A468**, 131 (1987).
[17] V. Zagrebaev and Yu. Penionzhkevich, Prog. Part. Nucl. Phys. **35**, 575 (1995).
[18] B. John, B. S. Tomar, A. Goswami, G. K. Gubbi, S. B. Manohar, and S. K. Kataria, Phys. Rev. C **56**, 2582 (1997).
[19] L. C. Northcliffe and R. F. Schilling, Nucl. Data, Sect. A **7**, 233 (1970).
[20] V. V. Volkov, in *Classical and Quantum Mechanical Aspects of Heavy Ion Collisions*, edited by H. L. Harney *et al.*, Lecture Notes in Physics Vol. 33 (Springer, Berlin, 1975), p. 254.
[21] D. J. Parker, J. J. Hogan, and J. Asher, Phys. Rev. C **35**, 161 (1987).
[22] A. Brondi, M. Kildir, G. La Rana, R. Moro, E. Vardaci, S. Pirrone, F. Porto, S. Sambataro, G. Politi, and P. Figvera, Phys. Rev. C **54**, 1749 (1996).
[23] A. Pagano, S. Aiello, E. DeFilippo, G. Lanzano, S. Lo Nigro, C. Milone, G. Blancato, G. Di Marco, and M. C. Mermaz, Phys. Rev. C **47**, 1170 (1993).
[24] J. P. Bondorf, F. Dickmann, D. H. E. Gross, and P. J. Siemens, J. Phys. (Paris), Colloq. **32**, C6 (1971).
[25] A. Gavron, Phys. Rev. C **21**, 230 (1985).